# 3D seismic imaging of the submarine slide blocks on the North Slope, Alaska

Shuvajit Bhattacharya[1], Sumit Verma[2], and Jonathan R. Rotzien[3]

**Abstract**

Submarine landslides are mass movements that transport sediment across the continental shelf to the deep ocean. This phenomenon happens when the shear stress exceeds the frictional resistance of the slope. We analyze a variety of seismic attributes to interpret large submarine slide blocks on the North Slope, Alaska. Results show that the slide blocks appear as mounds with scarps associated with them on the seismic section. The slide blocks vary in size, depending on their distance away from the shelf. The pattern of the slide blocks affects the overlying sedimentation.

**Geological feature:** Submarine slide blocks

**Seismic appearance:** Mound-like steep ramp and scarp characteristics on seismic sections; blocky and irregular features with sharp boundaries on the horizon slices and seismic attributes

**Features with similar appearance:** Mass-transport deposits; Remnant blocks; Reef deposits; Submarine channels; Gullies

**Formation:** Torok Formation

**Age:** Cretaceous

**Location:** North Slope, Alaska

**Seismic data:** Obtained from the Alaska Department of Natural Resources, Division of Oil and Gas, through the tax-credit program (State of Alaska, 2017, http://dggs.alaska.gov/gmc/seismic-well-data.php)

**Analysis tools:** Seismic attributes (such as coherent energy, Sobel-filter similarity, dip magnitude, and dip azimuth) and geobody extraction

## Introduction

Submarine slide blocks are found in ancient, recent, and modern-day environments (Robseco et al., 2014). Submarine landslides can be set into motion and generated due to rapid sedimentation, earthquakes, tsunamis, oversteepening of slopes, gas escape, and changes in the hydrodynamics conditions — basically any mechanism that causes sediment or sedimentary rock instability. Studies show that slides can involve upwards of 5500 $km^3$ of material, which can move great distances (Kneller et al., 2016). An understanding of the landslide distribution, internal architecture, composition, and geometry is important for assessing the integrity of the hydrocarbon prospects because they may serve as a top seal for underlying reservoirs, the main focus of this study. Giant submarine landslide deposits are present in the Gulf of Mexico, Greenland, Ireland, Norway, Brazil, Morocco, Nigeria, and New Zealand (Edwards, 2000; Huvenne et al., 2002; Apotria et al., 2004; Dykstra, 2005; Færseth and Sætersmoen, 2008; Alves and Cartwright, 2009; Dunlap et al., 2010; Gamboa et al., 2011; Alves, 2015; Rusconi, 2017; Cox et al., 2020). An understanding of modern-day slides also is important because these are potential geohazards. There are several areas in the Arctic where submarine slides may inhibit the release of gas from the gas hydrates and permafrost. Therefore,

[1]Formerly University of Alaska Anchorage, Alaska 99508, USA; presently University of Texas at Austin, Bureau of Economic Geology, Texas 78758, USA. E-mail: suva.geo@gmail.com (corresponding author).
[2]University of Texas Permian Basin, Odessa, Texas 79762, USA. E-mail: verma_s@utpb.edu.
[3]Basin Dynamics, Houston, Texas 77027, USA. E-mail: jon@basindynamics.com.
Manuscript received by the Editor 30 January 2020; revised manuscript received 6 May 2020; published ahead of production 10 July 2020.
This paper appears in *Interpretation*, Vol. 8, No. 4 (November 2020); p. 1–8, 7 FIGS.
http://dx.doi.org/10.1190/INT-2020-0038.1. 

the recognition and characterization of submarine slides and the associated traces pertaining to their transport are vital to geophysicists, geomorphologists, geotechnical engineers, and oceanographers involved in the exploration and production of natural resources and others working to understand marine sediment transport and depositional processes.

In this study, we interpret and analyze the massive submarine landslides present in the Cretaceous (Brookian-age) Torok Formation on the North Slope, Alaska, using 3D seismic data (Figure 1). Recently, there has been growing interest in exploration of the clastic reservoirs (i.e., Nanushuk and Torok) on the North Slope, Alaska (Houseknecht, 2019; Bhattacharya and Verma, 2020). The Nanushuk Formation is a clastic fluvial-deltaic-shelf succession, whereas the Torok Formation is its basinward equivalent. In terms of lithology, the Torok Formation is composed of shale, silty mudstone, and sandstone, deposited in the outer shelf, marine slope, and basin-floor fan environments, whereas the gamma-ray zone (GRZ) is an organic mudstone, which is one of the major source rocks on the North Slope (Houseknecht et al., 2009). Figure 2 shows the stratigraphic column in the study area. In terms of seismic stratigraphy based on the clinoform geometry, the Nanushuk topsets transition seaward into the foresets and bottomsets, which contain the age-equivalent Torok and GRZ formations (Houseknecht, 2019; Bhattacharya and Verma, 2020). We focus our study at the Torok and GRZ.

The Torok Formation consists of several geomorphological features, including slide deposits. There are several submarine slides in the subsurface of the North Slope, such as the Fish Creek slide, Dalton slide, Simpson canyon, and others. (Weimer, 1987; Homza, 2004). The Fish Creek slides, consisting of a group of slide blocks near the Harrison Bay, rank among the largest

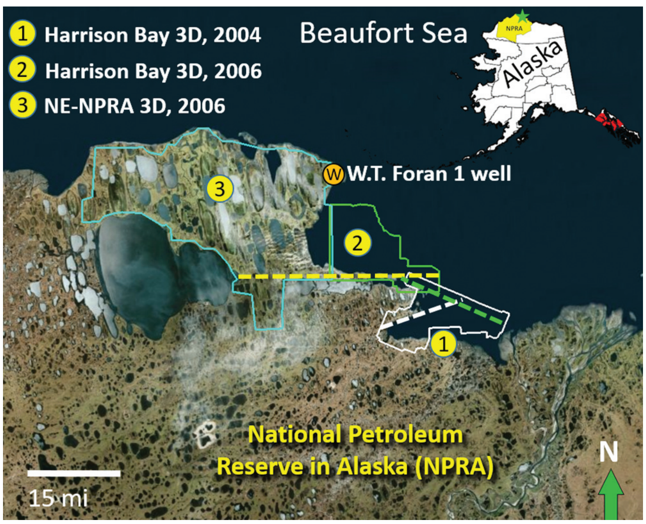


**Figure 1.** The study area on the North Slope, Alaska, with the three 3D seismic surveys used. The green star in the Alaska inset map shows the approximate location of the study area. The dark features on the surficial map show the lakes.

submarine landslides in size and spatial extent. Based on 2D seismic data, Weimer (1987) identifies that the Fish Creek slides are distributed over an area of approximately 1200 square miles (3500 square km). However, we cannot verify the exact geomorphic extent of these slides due to the limited spatial availability of 3D seismic surveys in the study area.

In this study, we use the Harrison Bay 3D seismic survey (acquired in 2004) on the North Slope, covering an area of 121 square miles (approximately 313.4 square km) (Figure 1). The survey has a nominal fold of 35 in 110 × 110 ft. (approximately 33.5 × 33.5 m) bins. In addition, we use two offset 3D seismic surveys, such as the Harrison Bay 3D (acquired in 2006) and NE-NPRA 3D (acquired in 2006), to provide an additional geologic interpretation of the scarp and submarine slide blocks in the basinal context. The total study area is approximately 954.02 square miles (approximately 2471 square km). We use geometric and amplitude attributes, such as dip azimuth, dip magnitude, Sobel-filter similarity (or coherence), and coherent energy (Bhatnagar et al., 2019). Although the root-mean-square (rms) amplitude is commonly used and available in most (or all) commercial software, we do not use it because it gets affected by noise. Coherent energy estimation involves singular value decomposition of the seismic data in different principal components, with different windows aligned along the structural dip (Bhattacharya and Verma, 2020). Although coherent energy attribute is similar to the rms amplitude, it is less susceptible to noise because the first few principal components of the seismic data contain the signal, whereas the latter components contain noise (Chopra and Marfurt, 2007).

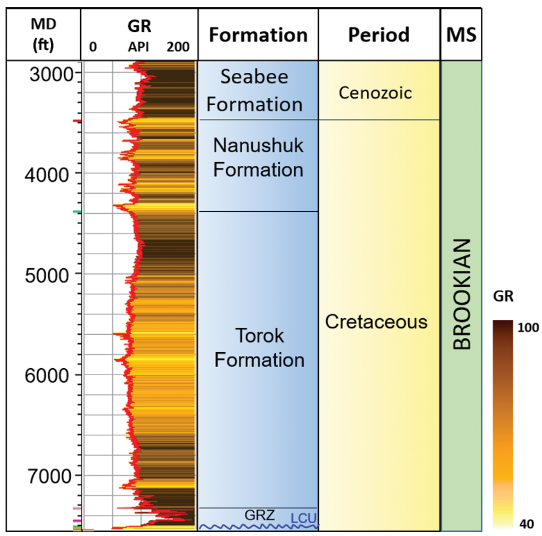


**Figure 2.** A stratigraphic column of the study area along with the gamma-ray (GR) curve from the W. T. Foran 1 well (shown in Figure 1). LCU corresponds to the Lower Cretaceous Unconformity, and MS corresponds to megasequence. The darker color in the GR log represents shale, whereas the light-yellow color represents sandstone. The Torok and GRZ are part of the Brookian sequence (Cretaceous).

We pick the base horizon ($N_1$) of the slide blocks and extract seismic attributes within a window of analysis above the horizon to better understand the slide geometry, internal architecture, and distribution (Figures 3, 4, and 5). In addition, we interpret the surfaces representing the inferred top of the mass-transport deposit (MTD) complex, infill facies, healed paleoseafloor, and clinoforms (such as the $N_2$–$N_7$ seismic horizons in Figures 3, 4, and 6). We generate 3D geobodies of the competent portion of the slide blocks in this area, using the coherent energy attribute (Figure 7).

Seismic attribute-based maps show that the slide blocks can be analyzed in detail. The seismic facies and internal character of the slide blocks vary between coherent and incoherent at places. The dimension of the slide blocks varies significantly. Larger and coherent slide blocks are present near the scarp in the Torok Formation (toward the shore in Figures 3 and 4), which is the area of origin of the slides. These organized slide blocks have a preferred orientation along the northwest–southeast. As we move away from the slope (more toward the distal portion of the basin), slide blocks become smaller, more incoherent, and randomly distributed. The presence of the GRZ shale below the Torok Formation introduces a velocity pushdown effect that deteriorates the seismic imaging of the sedimentary layers (many of which are reservoirs) stratigraphically below the slide blocks.

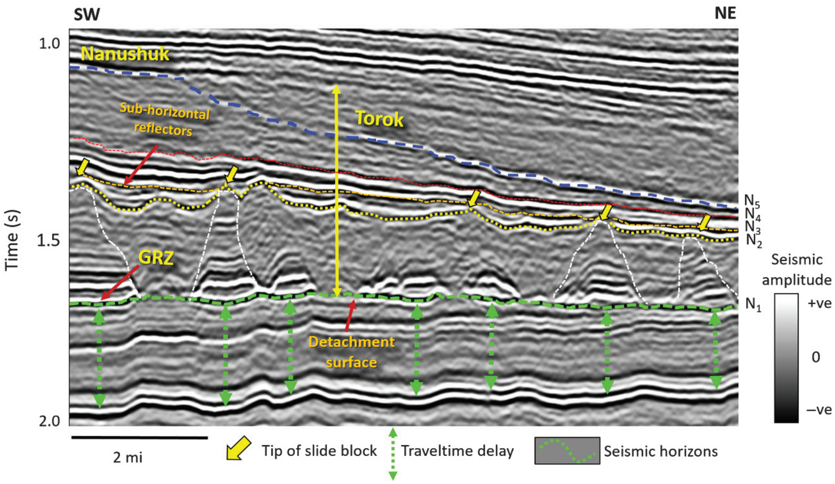


**Figure 3.** A seismic section along the southwest–northeast, showing the slide blocks present in this area (vertical exaggeration: 25). The yellow arrows show the tip of the inferred slide blocks, whereas the green double-headed arrows indicate the velocity pushdown effect due to the presence of the GRZ shale below the slide blocks. The $N_1$, $N_2$, $N_3$, $N_4$, and $N_5$ horizons indicate the bottom of the slide blocks (detachment surface), top of the MTD, infill onlap facies between blocks, healed paleoseafloor, and a Nanushuk-Torok clinoform, respectively. Note: The white dashed line in the Harrison Bay 3D seismic survey (2004) in Figure 1 indicates the location of the vertical seismic section.

## Seismic expression and interpretation

Based on our seismic data analysis, we find several important features of the slide blocks in our study area. First, the slide blocks are expressed on the seismic sections by the mound-like shape with steep ramp and scarp features, which are associated with axial lows that meet the detachment surface, marked by the $N_1$ horizon (Figure 3). Figure 4 shows a west–east seismic section, which goes through all three 3D seismic surveys. It shows the prominent scarp feature, responsible for the development of slide blocks. Slide blocks are larger close to the scarp, and these become smaller and thinner away from the scarp.

In terms of seismic attributes, low Sobel-filter similarity values characterize the external boundary of the slide blocks. The slide blocks take several external shapes, including trapezoidal, triangular, or cylindrical. In general, the slide blocks have sharp boundaries, indicated by the Sobel-filter similarity attribute (Figure 5a). Some of the slide blocks are narrow and steeply dipping, with significant amplitude contrasts against the outside material (i.e., onlap fill facies between the slide blocks). This is important because it reveals how the new topography created by the slide blocks has created accommodation for later sediment

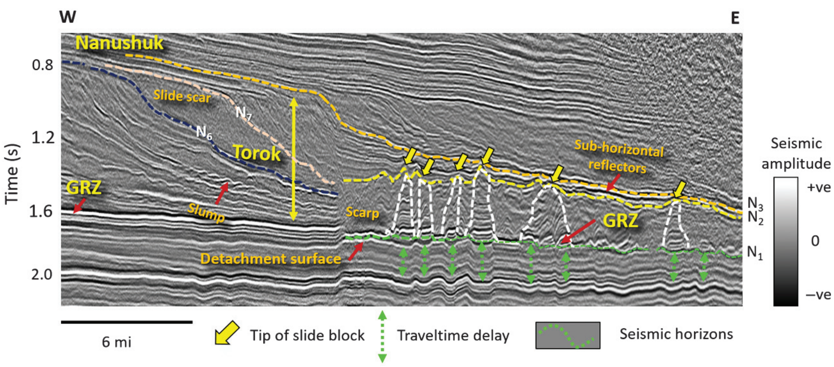


**Figure 4.** A seismic section along the west–east, showing the scarp and slide blocks present in this area (vertical exaggeration: 50). The yellow arrows show the tip of the inferred slide blocks, whereas the green double-headed arrows indicate the velocity pushdown effect below the slide blocks. Similar to Figure 2, the $N_1$ (detachment surface), $N_2$, and $N_3$ horizons are interpreted. The $N_6$ and $N_7$ horizons on the left side cannot be traced in the right because the scarp affects these. The detachment surface $N_1$ is not traced in the left because it is not present there. Note: The yellow dashed line in Figure 1 indicates the location of the vertical seismic section. This seismic line goes through all three 3D seismic surveys along the west–east.

gravity-flow deposits. The coherent energy attribute shows high amplitudes inside the slide blocks and low values surrounding them (Figure 5b). This observation indicates the slide blocks themselves are composed of similar geologic materials, with high acoustic impedance contrast. The dip-azimuth attribute modulated with dip magnitude shows that the organized, steeply dipping slide blocks (maximum dip: approximately 8°) are oriented mostly along the northwest–southeast, with the azimuth varying between approximately 280° and 320° (Figure 5c).

Overall, the slide block geometry transitions from coherent and organized to disorganized, with increasing distance basinward from the slope. However, looking at the seismic characteristics through the horizon slices of the slide blocks may reveal internal heterogeneities inside some of the slide blocks. Large and small slide blocks are present in the study area. In general, the width of the large coherent slide blocks varies between approximately 6000 and 8000 ft. (approximately 1829 and 2438 m), whereas the width of the smaller blocks is less than 2000 ft. (approximately 610 m). The large slide blocks mostly comprise parallel, subhorizontal reflectors with high amplitude and relatively small to no visible deformation inside them at seismic scale (Figure 3). The large slide blocks show some small-scale internal deformation at places. These slide blocks are also close to the shelf, compared to the smaller slide blocks in the distal portion of the basin (Figures 4 and 5). These large slide blocks mostly are arranged in a linear fashion along the northwest–southeast, parallel to the shelf edges. Figures 3 and 4 show that the base of such large slide blocks has parallel to near-parallel high-amplitude reflectors, not always at the top portion. Based on our experience and regional context, we think these features mostly represent competent (sandstone?) slide blocks at the base of the MTD that resisted internal deformation during mass movement and therefore retained their overall shape, whereas the coeval overlying and intervening infill material (less competent) experienced significant internal deformation (i.e., mudstone and possibly interbedded sandstone and mudstone). The Sobel-filter similarity attribute corendered with elevation of the top horizon ($N_2$) of the MTD shows the spatial distribution and overall geometry of the large competent slide blocks in plan view (Figure 6). Figure 6 also shows that the elevated portions of the MTD occur where competent slide blocks are present, which also implies that the thickness of the overall MTD system is high where large competent slide blocks are present. King et al. (2011) and Sharman et al. (2015) describe similar features in the outcrops in the deep-water clastic successions in the Taranaki basin (also referred to as the North Awakino MTD). The smaller slide blocks show internal deformation at places. Some of these smaller slide blocks appear to show bed-parallel shear and duplex features, and they rest on the top of the gliding surface. These smaller slide blocks also have slightly lower amplitudes than the larger slide blocks. Debrites are interpreted to be present between the slide blocks, with a chaotic and low-amplitude reflection pattern. The height of the debrites increases toward the large slide blocks.

The topography of the slide blocks creates a rugose paleoseafloor (Figures 3 and 4). We also observe some gentle folds (anticlines) on the top of these large slide blocks, which might have generated due to differential compaction of the sediment. The competent slide blocks also resisted compaction more than the flanking mud-rich debrite deposits during burial, which resulted in differential compaction between competent slide blocks and flanking strata that was able to maintain a rugose paleoseafloor. Ward et al. (2018) also observe this pattern in their study on the blocky MTD in Brazil. These topographic highs are surrounded by local depocenters above the debrites. The depocenters are filled with sediment, which show subhorizontal, semicontinuous to continuous seismic reflectors with high amplitude, onlapping against the walls of the slide blocks, marked by the $N_3$ seismic horizon (Figure 3). This thickness of the overlying infill facies varies in accordance with the underlying MTD top. In general, the thickness of the depocenters is high, where large slide blocks are absent, especially away from the slide blocks protruding above the

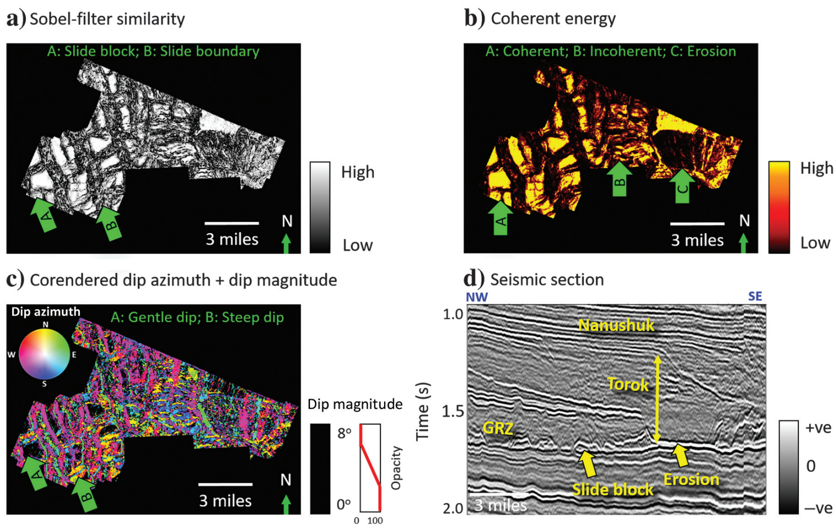


**Figure 5.** Computed seismic attributes, such as (a) Sobel-filter similarity, (b) coherent energy, (c) corendered dip azimuth and dip magnitude, and (d) a seismic section. The attributes are extracted from the base horizon of the slide blocks within a window of analysis above it. The bright colors in (c) indicate steeply dipping slide blocks, compared to darker colors. Note: The green dashed line in the Harrison Bay 3D seismic survey (2004) in Figure 1 indicates the location of the vertical seismic section (d).

paleoseafloor. Once the depocenters and the top of the slide blocks are completely filled with later sedimentation, the paleoseafloor starts healing, marked by the $N_4$ seismic horizon (Figure 3). Figure 3 also shows that the smaller slide blocks were completely buried before the deposition of the $N_3$ and $N_4$ seismic horizons, whereas the large slide blocks in the proximal region of the basin (toward the west and southwest) still had topographic relief until after the deposition of the $N_4$ seismic horizon. This is indicative of the role of MTD on the overlying sedimentation.

Although the genesis of the slide blocks is not in the current scope of the study, we think the en echelon geometries of the slide blocks might be indicative of progressive slope failure along the northwest–southeast, along which most of the slide blocks are arranged in a linear fashion. We show the evidence of the scarp in the western portion of the study area (Figure 4). Nixon et al. (2014), Bhattacharya and Verma (2019), Verma and Bhattacharya (2019), and Tatarin (2019) show evidence of a complex polyphase, extensional fault system on the North Slope. The structural grain in the basement is along the west–northwest-east–southeast, which was reactivated several times. Although we do not see numerous faults in the current study area, we do know of the existence of a normal fault and its splays, separating the Fish Creek platform from the Nechelik trough, a broad basement low (Kirschner and Rycerski, 1988; Homza, 2004). This might have triggered the slides. We do not have access to that offset 3D seismic survey used by Homza (2004). The alternate interpretation could be that these large slide blocks are indeed remnant blocks (Bhattacharya et al., 2020). Some of the features (e.g., strong amplitudes, large dimensions, sharp boundaries, and relatively small deformation) found inside the remnant blocks in other studies match the features found in the study area. However, we discard that interpretation because these features can be reconstructed like a jigsaw puzzle (after removing the gaps — interblock debrites), and smaller slide blocks are present away from the scarp, both of which are indicative of transport (Figures 4 and 6). There is some component of translation and rotation of the slide blocks being involved. In addition, some of the large slide blocks in Figure 4 show some internal deformation. We do not show the reconstructed image of the original slide blocks. The reconstruction process generally involves removing the interblock areas, juxtaposing the sections of the slide blocks, which were once laterally adjacent (Cox et al., 2020). If these large slide blocks along the northwest–southeast were remnants, smaller slide blocks away from the shore cannot cross them (Figure 6). In addition to geometric fit (i.e., jigsaw puzzle), the competent slide blocks have a similar width, which might not be possible if these slide blocks are just erosional remnants. Also, we find continuous, matching internal seismic reflection patterns inside the adjacent competent slide blocks, which indicates continuous depositional style and constituents across originally adjacent slide blocks. In addition, we do not really find the causal mechanism of forming these remnant highs. Based on our knowledge of the study area, there are no carbonate and salt deposits present, which created remnants in other basins around the world. Figure 6 shows the presence of smaller slide blocks in the distal portion away from the large slide blocks near the shore. This is indicative of the fact that the MTD system worked as one system. The large slide blocks with competent units at the base remained close to the shelf because they are heavy to move, whereas the slide blocks far from the shelf are smaller because they get transported and fragmented into smaller pieces with distance. The underlying GRZ shale provided the lubricated, smooth surface for the blocks to slide along. It is also possible that this underlying mudstone with high water content led to the development of a thin veneer of mud slurry above (below seismic resolution) that facilitated the movement of the slide blocks (Prior et al., 1984; Cox et al., 2020).

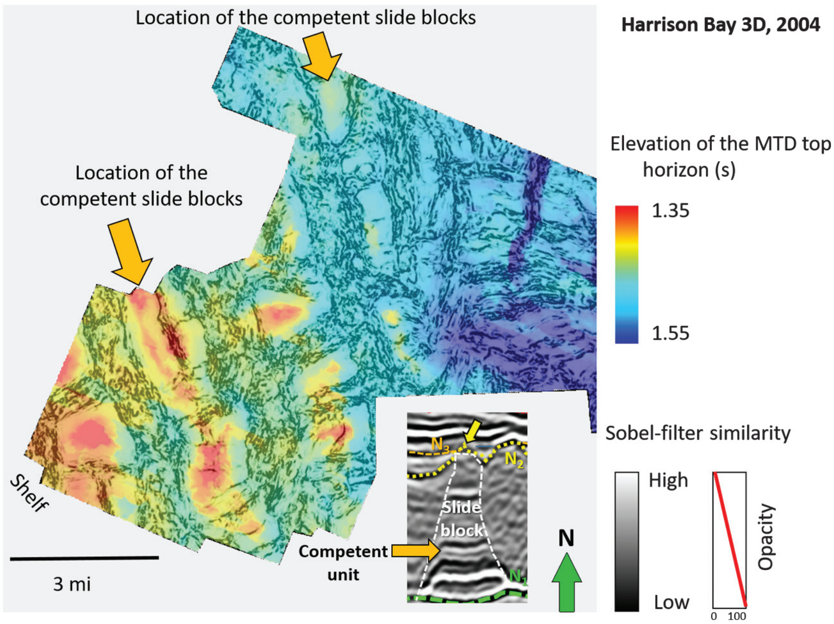


**Figure 6.** The plan view of the Sobel-filter similarity attribute corendered with elevation of the MTD top (the $N_2$ horizon in the time domain), showing the slide blocks with competent lithology at their base in the Harrison Bay 3D seismic survey (2004). The competent blocks are larger and present toward the shelf. The elevation map corresponds to the top of the inferred slide blocks (the $N_2$ horizon in Figure 3). The spatial extent of the map is smaller than the whole survey area because the $N_2$ seismic horizon (or the top of the MTD) is missing in the distal portion. The inset seismic section shows the geometry of an individual slide block with competent units at its base.

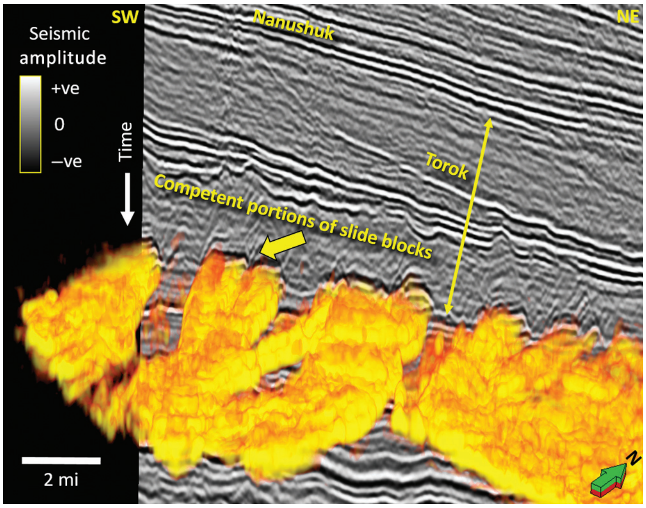


**Figure 7.** A 3D geobody of the competent portion of the irregular slide blocks extracted from the seismic data. The geobody shows the complexities of the slide blocks, in terms of their geometry, distribution, and connectivity. Detailed knowledge of the 3D distribution of the slide blocks could be useful in understanding the seal integrity of the reservoirs.

Second, most of the slide blocks overlie and downlap onto either the GRZ or the Lower Cretaceous unconformity. The presence of the GRZ shale increases the traveltime and introduces a velocity pushdown effect. The organic shale has a low interval velocity (approximately 8300–9000 ft/s, approximately 2530–2743 m/s), compared to the overlying and underlying layers. In general, the presence of organic matter (total organic carbon [TOC]) reduces the velocity. The TOC in the GRZ shale varies between 2 and 6 wt% (Peters et al., 2006). In this case, the organic-rich GRZ shale has a low velocity with respect to its overlying and underlying layers, which introduces the velocity pushdown effect (i.e., concave down appearance of seismic reflectors). The velocity pushdown phenomenon affects the imaging of all the underlying layers, which appear as concave downward reflectors. This is also significant in that it poses a challenge to interpreting the true architecture of the slide deposits and associated deep-water infill between the slide-affected environments — (1) the slide deposits themselves, (2) evacuated areas, and (3) zones showing evidence of slide transport. The two-way traveltime delay varies between 10 and 30 ms in this area. However, such effects are absent from the areas where the GRZ is either eroded or not deposited. Slide blocks are affected by large erosional features at places that are younger based on seismic reflector terminations (Figure 5d). Figure 5d shows another prominent scarp formed by the removal of materials in this position in the basin. The seismic expression of such erosional features is similar to a valley, which is bound by steep scarp surfaces against the slide blocks on both sides. In such cases, the later erosional event can impact the petroleum prospectivity of the underlying reservoirs in different ways, ranging from high-fidelity depth imaging to the breach of the top seal materials. Figure 7 shows the geobody of the competent portion of the slide blocks extracted from the coherent energy attribute, which displays their geometry and distribution pattern. Other than these main features, we observe polarity reversals and diffraction tails at places.

Many other geologic features may have similar expressions on seismic data, which could lead to erroneous interpretations. For example, these features may seem similar to carbonate reefs or mounds on seismic data, but they are not reefs or mounds based on the lithology of the rocks in the study area. Therefore, the context is important. These features are not rectangular or trellis drainages either. In the case of these drainages, the tributaries join the mainstream at approximately a right angle, which is indicative of a set of underlying fault or joint system, or even an alternating series of resistant and eroded rocks. The Connecticut River in the United States is one modern-day example of such drainages. Based on the seismic section displays, these features near the Torok slope are not channels (in the study area), marked by low values of Sobel-filter similarity. In addition, if these features were channels, they would show high coherent energy values along the channel on horizon slices due to the presence of sandstone, which these do not. Therefore, these geologic features are slide blocks, not carbonate mounds and rectangular/trellis drainage.

The scope of this study is about correctly recognizing slide blocks on seismic data; therefore, we limit the discussions to the seismic expressions of these features, not their detailed geologic evolution and implications. This approach would be helpful to other seismic interpreters while working on these interesting features because such features are found worldwide. Our future work will include a detailed geologic study of these slide blocks in the basinal context.

We compare and contrast similar-looking MTDs in seismic data published elsewhere in the world (Dunlap et al., 2010; Alves, 2015). Although there are geometric similarities of the features identified by Ward et al. (2018) in the Espirito Santos Basin in Brazil, we think our features have certain similarities to those in northwestern Greenland, in terms of genesis and processes (Cox et al., 2020).

## Conclusion

Submarine landslide blocks can be identified using an ensemble of seismic attributes, such as seismic amplitude, coherent energy, Sobel-filter similarity, dip magnitude, and dip azimuth. Based on the size, there are two different types of slide blocks present in the Torok Formation: (1) large slide blocks (width varying between approximately 1829 and 2438 m) with competent units at the base with little deformation and (2) small slide blocks (width less than approximately 610 m) with internal deformation. The majority of the large slide blocks have competent units near their base, compared to the top and flanking debrites. We think the

MTD moved toward the distal portion of the basin (along the east/northeast) as one system. The topography of the slide blocks creates a rugged paleoseafloor, with depocenters flanking the large slide blocks protruding above the paleoseafloor. The results obtained from our seismic interpretation show the relations between the slide blocks and the overlying depocenters. The depocenters are thick away from the protruding large slide blocks. In addition, it appears that the spatiotemporal distribution and overall geometry of the slide blocks controlled the sediment fairway between the blocks. Differential compaction allowed the formation of anticlinal features near the crest of the slide blocks before the complete healing of the paleoseafloor. If proper context and attributes are used, these features can be distinguished from other features, with similar appearances on seismic data, such as carbonate mounds and rectangular drainage. The lithology of the overlying and underlying sedimentary formations is also important because they can introduce artifacts. In this case, the presence of an organic-rich shale (i.e., GRZ) introduces the velocity pushdown effect, which deteriorates the imaging quality of the underlying reflectors and impacts accurate depth positioning of the boreholes.


## Acknowledgments

We thank the Alaska Department of Natural Resources, Division of Oil and Gas, for making the tax-credit 3D seismic data available to the University of Alaska Anchorage and University of Texas Permian Basin. We also thank Schlumberger for donating the Petrel software to the University of Alaska Anchorage and the University of Texas Permian Basin. We computed the seismic attributes using the AASPI consortium software. We thank F. Smit, T. Alvez, H. Bedle, and H. Di, whose comments helped to strengthen the manuscript.


## References


Alves, T. M., 2015, Submarine slide blocks and associated soft-sediment deformation in deep-water basins: A review: Marine and Petroleum Geology, **67**, 262–285, doi: 10.1016/j.marpetgeo.2015.05.010.

Alves, T. M., and J. A. Cartwright, 2009, Volume balance of a submarine landslide in the Espírito Santo Basin, offshore Brazil: Quantifying seafloor erosion, sediment accumulation and depletion: Earth and Planetary Science Letters, **288**, 572–580, doi: 10.1016/j.epsl.2009.10.020.

Apotria, T., R. Lindholm, W. Metner, M. Eze, D. Gunn, J. Geslin, P. Rumelhart, F. Goulding, and S. Mitchell, 2004, Volume interpretation of shelf collapse processes and Biafra 'disturbed' reservoirs, Eastern Niger Delta Joint Venture: AAPG International Conference, Cancun, Mexico.

Bhatnagar, P., S. Verma, and R. Bianco, 2019, Geomorphologic character of an Upper Leonardian mass transport deposit, Midland Basin: insights from 3D seismic data: Interpretation, **7**, no. 4, SK19–SK32, doi: 10.1190/INT-2019-0036.1.

Bhattacharya, S., M. Tian, J. Rotzien, and S. Verma, 2020, Application of seismic attributes and machine learning for imaging submarine slide blocks on the North Slope, Alaska: 90th Annual International Meeting, SEG Technical Program, Expanded Abstracts, doi: 10.1190/segam2020-3426887.1.

Bhattacharya, S., and S. Verma, 2019, Application of volumetric seismic attributes for complex fault network characterization on the North Slope, Alaska: Journal of Natural Gas Science & Engineering, **65**, 56–67, doi: 10.1016/j.jngse.2019.02.002.

Bhattacharya, S., and S. Verma, 2020, Seismic attribute and petrophysics-assisted interpretation of the Nanushuk and Torok formations on the North Slope, Alaska: Interpretation, **8**, no. 2, SJ17–SJ34, doi: 10.1190/INT-2019-0112.1.

Chopra, S., and K. J. Marfurt, 2007, Seismic attributes for prospect identification and reservoir characterization: SEG, doi: 10.1190/1.9781560801900.

Cox, D. R., M. Husse, A. M. W. Newton, P. Gannon, and J. Clayburn, 2020, Slip sliding away: Enigma of large sandy blocks within a gas-bearing mass transport deposit, offshore northwestern Greenland: AAPG Bulletin, **104**, 1011–1043, doi: 10.1306/10031919011.

Dunlap, D. B., L. J. Wood, C. Weisenberger, and H. Jabour, 2010, Seismic geomorphology of offshore Morocco's east margin, Safi Haute Mer area: AAPG Bulletin, **94**, 615–642, doi: 10.1306/10270909055.

Dykstra, M., 2005, Dynamics of sediment mass-transport from the shelf to the deep sea: Ph.D. thesis, University of California, Santa Barbara, California, 152 p.

Edwards, M. B., 2000, Origin and significance of retrograde failed shelf margins; tertiary northern Gulf Coast Basin: Gulf Coast Association of Geological Societies Transactions, **50**, 81–93.

Færseth, R. B., and B. S. Sætersmoen, 2008, Geometry of a major slump structure in the Storegga slide region offshore western Norway: Norwegian Journal of Geology, **88**, 1–11.

Gamboa, D., T. Alves, and J. Cartwright, 2011, Distribution and characterization of failed (mega) blocks along salt ridges, southeast Brazil: Implications for vertical fluid flow on continental margins: Journal of Geophysical Research: Solid Earth, 116.

Homza, T. X., 2004, A structural interpretation of the Fish Creek Slide (Lower Cretaceous), northern Alaska: AAPG Bulletin, **88**, 265–278, doi: 10.1306/10270303029.

Houseknecht, D. W., 2019, Petroleum systems framework of significant new oil discoveries in a giant Cretaceous (Aptian–Cenomanian) clinothem in Arctic Alaska: AAPG Bulletin, **103**, 619–652, doi: 10.1306/08151817281.

Houseknecht, D. W., K. J. Bird, and C. J. Schenk, 2009, Seismic analysis of clinoform depositional sequences and shelf-margin trajectories in Lower Cretaceous (Albian) strata, Alaska North Slope: Basin Research, **21**, 644–654, doi: 10.1111/j.1365-2117.2008.00392.x.

Huvenne, V. A. I., P. F. Croker, and J.-P. Henriet, 2002, A refreshing 3-dimensional view of an ancient sediment collapse and slope failure: Terra Nova, **14**, 33–40, doi: 10.1046/j.1365-3121.2002.00386.x.

King, P. R., B. R. Ilg, M. J. Arnot, G. H. Browne, L. J. Strachan, M. P. Crundwell, and K. Helle, 2011, Outcrop and seismic examples of mass-transport deposits from a Late Miocene deepwater succession, Taranaki Basin, New Zealand, *in* R. C. Shipp, P. Weimer, and H. W. Posamentier, eds., Mass-transport deposits in deepwater settings: Society for Sedimentary Geology, Special Publication 96, 311–348.

Kirschner, C. E., and B. A. Rycerski, 1988, Petroleum potential of representative stratigraphic and structural elements in the National Petroleum Reserve in Alaska, *in* G. Gryc, ed., Geology and exploration of the National Petroleum Reserve in Alaska: U.S. Geological Survey Professional Paper 1399, 191–208.

Kneller, B., M. Dykstra, L. Fairweather, and J. P. Milana, 2016, Mass-transport and slope accommodation: Implications for turbidite sandstone reservoirs: AAPG Bulletin, **100**, 213–235, doi: 10.1306/09011514210.

Mosher, D. C., C. Shipp, L. Moscardelli, J. Chaytor, C. Baxter, H. Lee, and R. Urgeles (Eds.), 2010, Submarine mass movements and their consequences: 4th International Symposium: Springer.

Nixon, C. W., D. J. Sanderson, S. J. Dee, J. M. Bull, R. J. Humphreys, and M. H. Swanson, 2014, Fault interactions and reactivation within a normal fault network at Milne Point, Alaska: AAPG Bulletin, **98**, 2081–2107, doi: 10.1306/04301413177.

Peters, K., L. Magoon, K. Bird, Z. Valin, and M. Keller, 2006, North Slope, Alaska: Source rock distribution, richness, thermal maturity, and petroleum charge: AAPG Bulletin, **90**, 261–292, doi: 10.1306/09210505095.

Prior, D. B., B. D. Bornhold, and M. W. Johns, 1984, Depositional characteristics of a submarine debris flow: Journal of Geology, **92**, 707–727, doi: 10.1086/628907.

Robesco, M., F. J. Hernández-Molina, D. V. Rooij (UGent), and A. Wåhlin, 2014, Contourites and associated sediments controlled by deep-water circulation processes: State-of-the-art and future considerations: Marine Geology, **352**, 111–154.

Rusconi, F. J., 2017, 3D seismic interpretation of a Plio-Pleistocene mass transport deposit in the deepwater Taranaki Basin of New Zealand, http://scholarworks.uark.edu/etd/2583

Sharman, G., S. A. Graham, L. U. Masalimova, L. E. Shumaker, and P. R. King, 2015, Spatial patterns of deformation and paleoslope estimation within the marginal and central portions of a basin-floor mass-transport deposit, Taranaki Basin, New Zealand: Geosphere, **11**, 266–306, doi: 10.1130/GES01126.1.

State of Alaska, Department of Natural Resources, Division of Oil & Gas, 2017, AS 43.55 Exploration Tax Credit Project, http://dog.dnr.alaska.gov/Information/GeologicalAndGeophysicalData

Tatarin, T., 2019, Extension history, fault evolution, and structural inheritance along the multiphase Beaufort rifted margin, Northern Alaska: M.S. thesis, University of Alaska Anchorage.

Verma, S., and S. Bhattacharya, 2019, Delineation of complex fault network North Slope, Alaska using seismic attributes: 89th Annual International Meeting, SEG Technical Program, Expanded Abstracts, 1893–1897, doi: 10.1190/segam2019-3214607.1.

Ward, N. I. P., T. M. Alves, and T. G. Blenkinsop, 2018, Submarine sediment routing over a blocky mass-transport deposit in the Espırito Santo Basin, SE Brazil: Basin Research, **30**, 816–834, doi: 10.1111/bre.12282.

Weimer, P., 1987, Seismic stratigraphy of three areas of lower slope failure, Torok Formation, northern Alaska, *in* I. Tailleur and P. Weimer, eds., Alaskan North Slope geology: Pacific Section SEPM and the Alaska Geological Society, 481–496.

---

Biographies and photographs of the authors are not available.